Antiviral Research 204 (2022) 105363

Contents lists available at ScienceDirect

Antiviral Research

journal homepage: www.elsevier.com/locate/antiviral

Liver biopsy of chronic hepatitis B patients indicates HBV integration profile may complicate the endpoint and effect of entecavir treatment

Mingyuan Zhang [a,d], Haikun Zhang [b], Xiaoming Cheng [c], Xiaomei Wang [a,d], Hongqin Xu [a,d], Xiuzhu Gao [a,d], Ruihong Wu [a,d], Dake Zhang [b,**], Yuchen Xia [c,***], Junqi Niu [a,d,*]

[a] Department of Hepatology, First Hospital of Jilin University, Changchun, 130021, PR China
[b] Key Laboratory of Biomechanics and Mechanobiology, Ministry of Education, Beijing Advanced Innovation Center for Biomedical Engineering, School of Engineering Medicine, Beihang University, Beijing, 100083, PR China
[c] State Key Laboratory of Virology and Hubei Province Key Laboratory of Allergy and Immunology, Institute of Medical Virology, School of Basic Medical Sciences, Wuhan University, Wuhan, PR China
[d] Center for Pathogen Biology and Infectious Diseases, Department of Hepatology, Key Laboratory of Organ Regeneration & Transplantation of Ministry of Education, The First Hospital of Jilin University, Changchun, 130061, PR China

ARTICLE INFO

Keywords:
Hepatitis B
Integration
Antiviral therapy
Hepatitis B surface Antigen

ABSTRACT

Aims: Viral integration profiles attract increased interest in the study of HBV-related hepatocellular carcinoma (HCC), but their features in the early stage of infection and changes due to antiviral treatments remain largely unknown.

Methods: Liver biopsies and paired blood samples were obtained from HBeAg-positive patients before and after 48 weeks of entecavir treatment, and a probe-based capture strategy was applied for analyzing the HBV integrations in these samples. Serum HBV markers, including viral DNA, pgRNA, and HBsAg, were longitudinally assessed.

Results: Entecavir treatment successfully reduced the levels of ALT, AST, and HBV serological markers (HBeAg, HBV pgRNA, and HBV DNA) in all patients (<40 years old). As expected, HBV integrations contributed to HBsAg production, with the total number of integrations positively correlated with serum HBsAg level ($r = 0.47$, $P = 0.04$). Along with repressed HBV replication, the number of viral integrations in liver biopsies decreased by about 1.94-fold after ETV treatment, with viral breakpoints significantly enriched within nt 1600–1900 of the HBV genome. No recurrent events were observed both at baseline and after treatment for the same individual, and only one same integration was found in two patients. Unlike in tumors, integrations in CHB biopsies seemed to have no chromosomal preference. Moreover, CHB integrations demonstrated lower enrichment scores for open active states than tumors, such as DNase, TssA, and ZNF/Rpts, and the scores reduced after ETV treatment. The antiviral therapy led to the disappearance of the enrichment tendency of integrations in both open chromatin and heterochromatin regions.

Conclusion: Reduced HBV replications by the nucleoside analogue may lead to decreased viral integrations in the liver, and those contributing to the HBsAg production may consistently occur. The pattern of HBV integration after ETV treatment is more random and irregular, which may contribute to a reduced risk of liver cancer due to antiviral treatment.

* Corresponding author. Key Laboratory of Organ Regeneration & Transplantation of Ministry of Education, The First Hospital of Jilin University, Changchun, 130061, PR China.
** Corresponding author.
*** Corresponding author. Institute of Medical Virology, School of Basic Medical Sciences, Wuhan University, Wuhan, China.
E-mail addresses: mingyuanzhang@jlu.edu.cn (M. Zhang), hkZhang@buaa.edu.cn (H. Zhang), xiaoming.cheng@whu.edu.cn (X. Cheng), xiaomeiwang@jlu.edu.cn (X. Wang), hongqinxu@jlu.edu.cn (H. Xu), xiuzhugao@jlu.edu.cn (X. Gao), wuruihong@jlu.edu.cn (R. Wu), dakezhang@buaa.edu.cn (D. Zhang), yuchenxia@whu.edu.cn (Y. Xia), junqiniu@jlu.edu.cn (J. Niu).

https://doi.org/10.1016/j.antiviral.2022.105363
Received 30 March 2022; Received in revised form 1 June 2022; Accepted 9 June 2022
Available online 13 June 2022

1. Introduction

Abbreviations

HBV	hepatitis B virus
HBsAg	hepatitis B surface antigen
HBeAg:	hepatitis B e antigen
HBV-pgRNA	HBV pregenomic RNA
NTCP	sodium taurocholate cotransporting polypeptide;
HCC	hepatocellular carcinoma
CHB	chronic hepatitis B infection
dsDNA	double-stranded DNA
dslDNA	double-stranded linear DNA
NUCs	nucleotide analogs
anti-HBs	hepatitis B surface antibody
anti-HBe	hepatitis B e antibody
anti-HBc	hepatitis B core antibody
ALT	alanine transaminase
ULN	upper limit of normal
HCV	hepatitis C virus
HDV	hepatitis D virus
HIV	human immunodeficiency virus
qPCR	quantitative polymerase chain reaction
CNV	copy number change
SNVs	single nucleotide variants
TERT	telomerase reverse transcriptase

Hepatitis B virus (HBV) infection is a public health problem that seriously threatens human health. In 2019, 296 million individuals worldwide were diagnosed with chronic hepatitis B (CHB), and 1.5 million individuals are newly infected with HBV annually (Razavi, 2020). A meta-analysis shows that the HBV infection rate in China was 6.89% (95%CI: 5.84–7.95%) between 2013 and 2017 (Wang et al., 2019). It is of great significance to prevent CHB from developing into liver cirrhosis and liver cancer.

HBV virions invade the hepatocyte cytoplasm through specific interactions with sodium taurocholate cotransporting polypeptide (NTCP). HBV DNA can be integrated into the hepatocyte genome, which is not essential for the viral replication cycle, but due to the ligation of HBV double-stranded linear DNA (dslDNA) into double-strand breaks in the host genome (Beck and Nassal, 2007; Block et al., 2007; Kim et al., 2021; Zhang et al., 2021). DslDNA is considered to be a byproduct of HBV replication (Tu et al., 2017) and cannot produce pgRNA after its integration into the host genome and thereby cannot complete viral replication. HBV integration can occur at all stages of chronic infection (Lee et al., 1999; Sung et al., 2012). Since integrated HBV DNA existed in over 85% of HBV-associated HCCs (Lin et al., 2021; Ruan et al., 2019), oncogenic roles of HBV integrations have been widely explored. Integrated HBV DNA may be responsible for chromosome instability or aberrant gene expression of the host genome. In HCC tissues, HBV integration often interrupts genomic regions, most likely conferring survival benefits to infected cells. However, they are randomly distributed in nuclear genomes of non-tumor tissues (Mason et al., 2010).

Viral integrations harboring S and part of the HBx sequences can produce either HBsAg or a truncated, but potentially functional, HBx (Martinez et al., 2021; Tu et al., 2018; Wooddell et al., 2017). HBsAg and HBx have long been considered to be involved in tumorigenesis of infected hepatocytes (Pollicino and Caminiti, 2021). Furthermore, HBsAg clearance is the ideal endpoint for antiviral treatment, which can be confounded by HBV integrations (Block et al., 2013; Chinese Society of Infectious Diseases and Chinese Society of Hepatology, 2019; European Association for the Study of the Liver. Electronic address and European Association for the Study of the, 2017; Song et al., 2021; Terrault et al., 2016). Patients who had HBV DNA cleared naturally after 3–10 years may still have high serum HBsAg levels (Hu et al., 2018). Therefore, viral protein expression due to HBV integration attracts much interest. Currently, antiviral treatments have been known to reduce the occurrence of HBV-related HCC (Hsu et al., 2020), but the speculated effects on integration events due to NUCs remain unclear.

Traditional HBV integration detections rely on polymerase chain reaction (PCR) amplification, such as Alu-HBV PCR (Murakami et al., 2005; Tamori et al., 2005). With the rapid development of next-generation sequencing (NGS), the resequencing of HCC genomes has identified HBV integration sites interrupting tumor-related genes (Fujimoto et al., 2012; Sung et al., 2012; Zhao et al., 2016). However, the high cost of whole-genome sequencing prevents further attempts, and the viral probe-based capture strategy is a popular strategy for enriching integrated HBV DNA for a significantly increased sensitivity and achieving deep-sequencing of these sites at a small sequencing volume (Chen et al., 2020). With this strategy, we characterized HBV integrations in liver biopsies of patients with CHB before and after anti-viral treatment to investigate the effects of ETV on integration frequencies along with repressed HBV replications, such as those commonly observed in tumors. Additionally, the strategy helped assess whether the short-term pressure during the treatment may lead to integration selection, such as those commonly observed in tumors.

2. Materials and methods

2.1. Study participants and sample collection

Ten HBeAg-positive, non-cirrhotic patients with CHB were recruited from a multi-center, randomized, controlled clinical trial between March 2015 and December 2017 (Clinical Trials.gov identifier: NCT03546530). All recruited patients completed the full course of 48 weeks of treatment and had paired liver biopsies at baseline and week 48. Additionally, serial serum tests were performed during treatment. These patients were treated with entecavir (Bristol-Myers Squibb Company, US) at a dose of 0.5 mg/daily for 48 weeks. The inclusion and exclusion criteria are provided in the supplementary files.

The research protocol was approved by the Ethics Committee of the First Hospital of Jilin University and other participating institutions (#2014-224). According to the Helsinki Declaration of 1975, all patients provided written informed consent.

2.2. Standard laboratory assessments

Peripheral serum samples obtained from all patients at baseline, week 4, week 12, week 24, week 36, and week 48 during treatment were stored at −80 °C for virological analyses. Paired liver biopsies were collected at baseline and week 48; they were snap-frozen in liquid nitrogen before integration capture. The details of laboratory procedures are described in supplementary materials and previous reports (Wang et al., 2020, 2021).

2.3. Probe design and sequencing experiments

The probe-based capture strategy to enrich integrated HBV DNA was verified in blood and tumor tissues from patients with HBV infection in our previous study (Chen et al., 2020). Briefly, viral probes (baits) for liquid capture were obtained from iGeneTech Bioscience (design.igen

etech.com, China), and the design adopted the tilling strategy across the whole HBV genome. For each sample, 200 ng genomic DNA was sheared by an ultrasonic DNA disruptor (Biorupter, Diagenode, Belgium) into fragments at 150–200 bp. The ends of the DNA fragment were repaired, and the Illumina Adaptor was added (Fast Library Prep Kit, iGeneTech, Beijing, China). Thereafter, the DNA fragments were conducted using the standard capture assay protocol, which was included in the TargetSeq Enrichment Kit (Target DNA Capture, iGeneTech Bioscience). After the sequencing library was constructed, the whole exons were captured with AIExome Enrichment Kit V1 (iGeneTech, Beijing, China) and sequenced on the Illumina platform (Illumina, San Diego, CA) with 150 base paired-end reads.

2.4. Breakpoint detection, annotation, and visualization of HBV integration

After base calling, paired-end reads were trimmed using Trimmomatic (v0.36) to remove low-quality bases and adapter sequences with parameters "SLIDINGWINDOW:4:15 MINLEN:36". A reference genome was constructed by adding the HBV genome (HBV genotype B and C) into the human reference genome (hg19). Filtered paired-end reads were mapped to the reference genome with the BWA-MEM algorithm (v0.7.17). After alignment, PCR duplicated read-pairs were removed using the Mark Duplicates function included in the Picard software (v2.22.8). A breakpoint was identified if a part of the reads aligned to the HBV genome and the other part aligned to the human genome. The candidate integration events were further filtered by at least 10 non-redundant split reads. Paired breakpoints were defined as two breakpoints located within 20 kb in the human genome.

2.5. Annotation and visualization of HBV integration

The R package ChIP seeker was applied to annotate the genomic region of the breakpoints. Each breakpoint was annotated for each RefSeq transcript obtained from ENSEMBL GRCh37, and the R package GenVisR was used for the waterfall map of the recurrent integration events located in the genes. Gene ontology (GO) analysis was performed using the R package clusterProfiler (Wu et al., 2021). The human genome browser by the University of California Santa Cruz (UCSC) and roadmap were used for the visualization of genomic features near the integration sites. The HBV integration sites of the tumor were reported by previous studies (28). DNase data were obtained from ENCODE, and ChromHMM epigenetic marks were downloaded from the roadmap. The active state included active TSS proximal promoter states (TssA, TssAFlnk), transcribed state at the 5′ and 3′ end of genes showing both promoter and enhancer signatures (TxFlnk), actively transcribed states (Tx, TxWk), enhancer states (Enh, EnhG), and states associated with Zn finger protein genes (ZNF/Rpts). The inactive states included constitutive heterochromatin (Het), bivalent regulatory states (TssBiv, BicFlnk, EnhBiv), repressed polycomb states (ReprPC, ReprPCWk), and quiescent state (Quies). Enrichment for genomic regions and epigenetic features was determined empirically using the GAT program.

2.6. Statistical methods

All the workflow and statistical analyses, including breakpoint calling, Spearman correlation test, and Wilcoxon rank-sum test, were performed using Perl and R. Clinical data are expressed as the mean ± standard deviation (SD). Statistical analyses of biological replicates were performed using the student's unpaired two-tailed *t*-test.

3. Results

3.1. The amount of HBV integrations in liver biopsies of CHB patients before and after ETV treatment contributes to HBsAg levels

For 10 patients with CHB, including six males and four females enrolled in this study, blood and liver tissue samples before and after ETV treatment were collected (Study design in Fig. 1A, Methods). For blood samples, Patients 1–5 had increased serum HBsAg level, and Patients 6–10 had decreased HBsAg level after 48 weeks of treatment (Table S1). Compared to patients with decreased HBsAg level, those with increased HBsAg level had lower levels of HBV DNA (7.0 ± 1.3 vs. 8.1 ± 0.2 log10 IU/mL, $P < 0.05$) and HBV pgRNA (7.2 ± 0.9 vs. 9.1 ± 0.4 log10 IU/mL, $P < 0.05$). No differences were observed in gender, age, ALT, HBsAg, or anti-HBe ($P > 0.05$). Additionally, all patients had anti-HBs negative test results before and after treatment (Table S1).

For liver biopsies, we obtained over 10 million raw sequencing reads for each sample on average using the HBV DNA capture assay. Across all the 20 liver biopsy samples, 1069 HBV integrations were identified with their numbers varying from 7 to 280 (mean, 51). The integration quantity fluctuated more obviously in samples before the treatment, and Patient 10 even had 280 integrations at baseline. After ETV treatment, total HBV integrations reduced by 1.94-fold, possibly due to limited dslDNA for integration benefiting from suppressed HBV replication. However, for each patient, the tendency was not consistent, and no significant difference was detected for integrations in paired biopsies ($P = 0.1724$, Paired *t*-test, Table S1).

Particularly, among all virological markers, HBV integration quantity only positively correlated with the level of HBsAg (Spearman correlation coefficient = 0.47, $P = 0.035$, Fig. 1B). Altogether, seven patients showed the same change tendency of integration events and HBsAg levels before and after ETV treatment; whereas three patients, Patients 4, 5, and 8, did not show such tendency (Fig. 1C). For instance, after treatment, Patient 8 had integrations increased from 22 to 38 but had a decreased serum HBsAg level from 4.4 to 3.32 log IU/mL. The viral protein-coding ability of viral integrations might have complicated the correlation. We further predicted the S protein-coding ability for integrations with both breakpoints detected (iHBV-S, Fig. 1C, method details see (32). Briefly, we first paired the two neighbor breakpoints for one integration to predict the viral integrants according to both breakpoints in the HBV genome (28/713 in patients with CHB without therapy and 54/363 in patients with CHB after 48 weeks of anti-viral treatment; Table S2). For integrants harboring the S gene, iHBV-S, almost all patients with increased HBsAg level (80%, 4/5) had at least one detected at week 48. iHBV-S was observed in only two patients with decreased HBsAg level after the treatment, with serum HBsAg over 3.32 log10 IU/mL, which was higher than those in patients without iHBV-S detected. It consisted of previous observations of HBV integrations contributing to HBsAg production. Additionally, the level of HBeAg and HBV DNA did not correlate with HBV integrations ($P > 0.05$, Spearman correlation test, Fig. 1B).

3.2. No recurrent integrations identified in CHB patients before and after ETV treatment

Integrations randomly occur in the early stage of infection, and these affected hepatocytes most likely do not have survival benefits to expand into large clones. Theoretically, biopsies of the same patient with CHB collected at two different time points are likely to sample different hepatocyte populations and obtain distinct integrations. As expected, no recurrent HBV integrations existed before and after treatment in the liver biopsy samples of the same patient.

For all the HBV integrations, only one at the same genomic position (chr7: 105741915, hg19) was found in different individuals (Patient 2 at baseline and Patient 8 after treatment; Table S2, Fig. 1C). Genomic annotation revealed that integrations directly interrupted 411 genes in

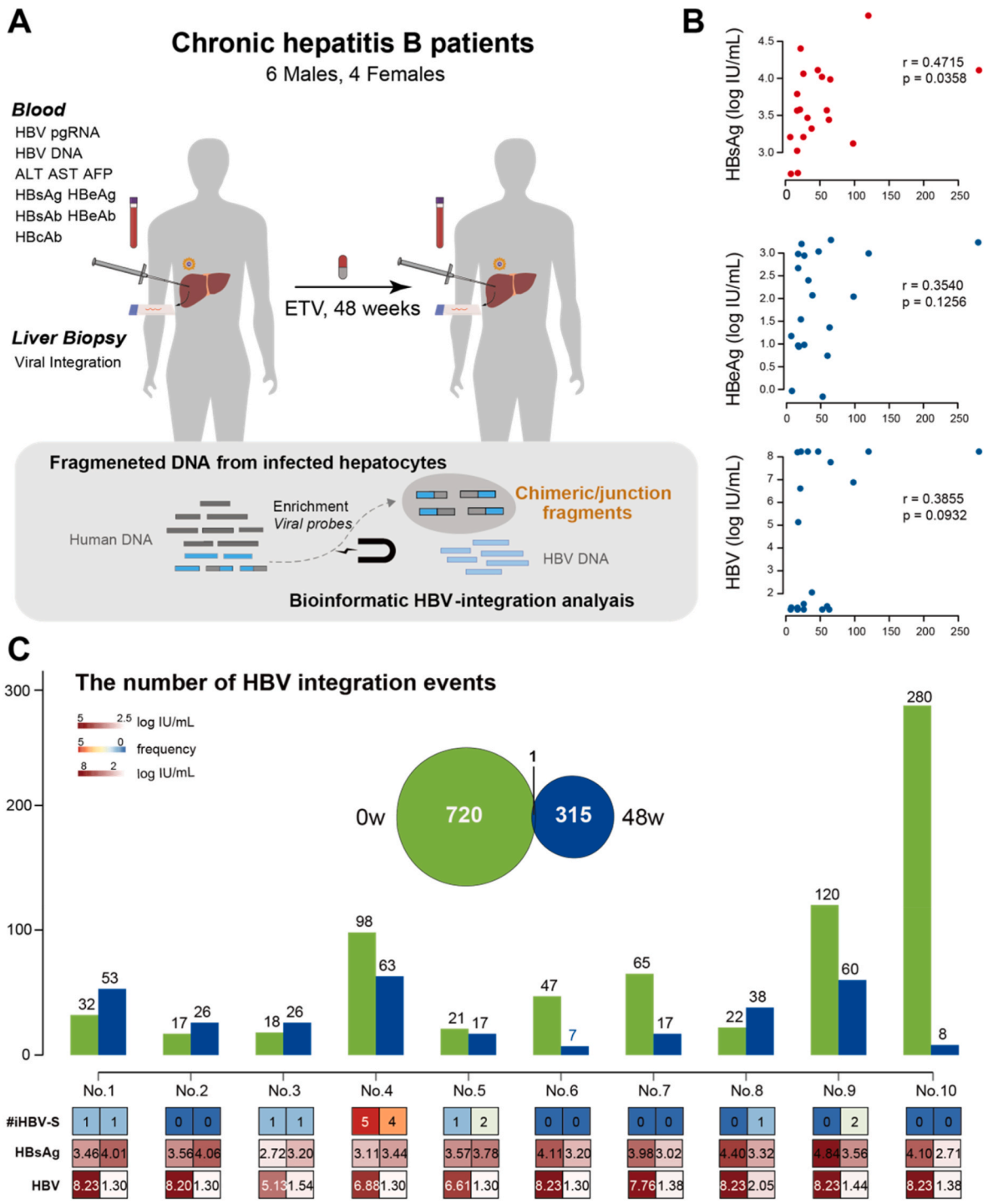

Fig. 1. The viral probe strategy reveals the relationship between HBV integration sites and HBsAg level of CHB patients before and after ETV treatment. (A) Experimental schematic for identifying HBV integration sites of CHB patients before and after ETV treatment. **(B)** The relationship between the number of integration sites and serum virological indicators, including HBsAg (log IU/ml), HBeAg (log IU/ml) and HBV DNA (log IU/ml). Correlation values and *P* values were determined by Spearman correlation test. **(C)** The barplot and heatmap display the number of HBV integration sites and HBV virological markers for CHB patients before and after ETV treatment. iHBV-s: paired integration event harboring the intact S gene (nt 155–835).

20 samples (Fig. 2A), which are mainly associated with synaptic transmission and signal transduction (Gene Ontology enrichment, Method). The top three enriched biological processes were modulation of chemical synaptic transmission, regulation of trans-synaptic signaling, and cell junction assembly ($P < 0.05$, Fig. 2B). Particularly, viral integrations could be observed to interrupt the same gene in tissues collected from the same individual at two different time points, while at distinct genomic positions. Evidence came from two cases: *CLVS1* in Patient 1 (baseline: chr8: 62412274, after 48 weeks: chr8: 62118869, Table 1) and *DOCK3* in Patient 9 (baseline: chr3: 51070499, after 48 weeks: chr3:50985393, Table 1). Within the 20 kb surrounding region of integrations, 739 genes were affected, most of which were enriched in the modulation of chemical synaptic transmission and regulation of trans-synaptic signaling (Fig. S1). Among them, *FTCD* and *COL6A2* in Patient 8 were affected by different integrations before and after treatment (Table 1).

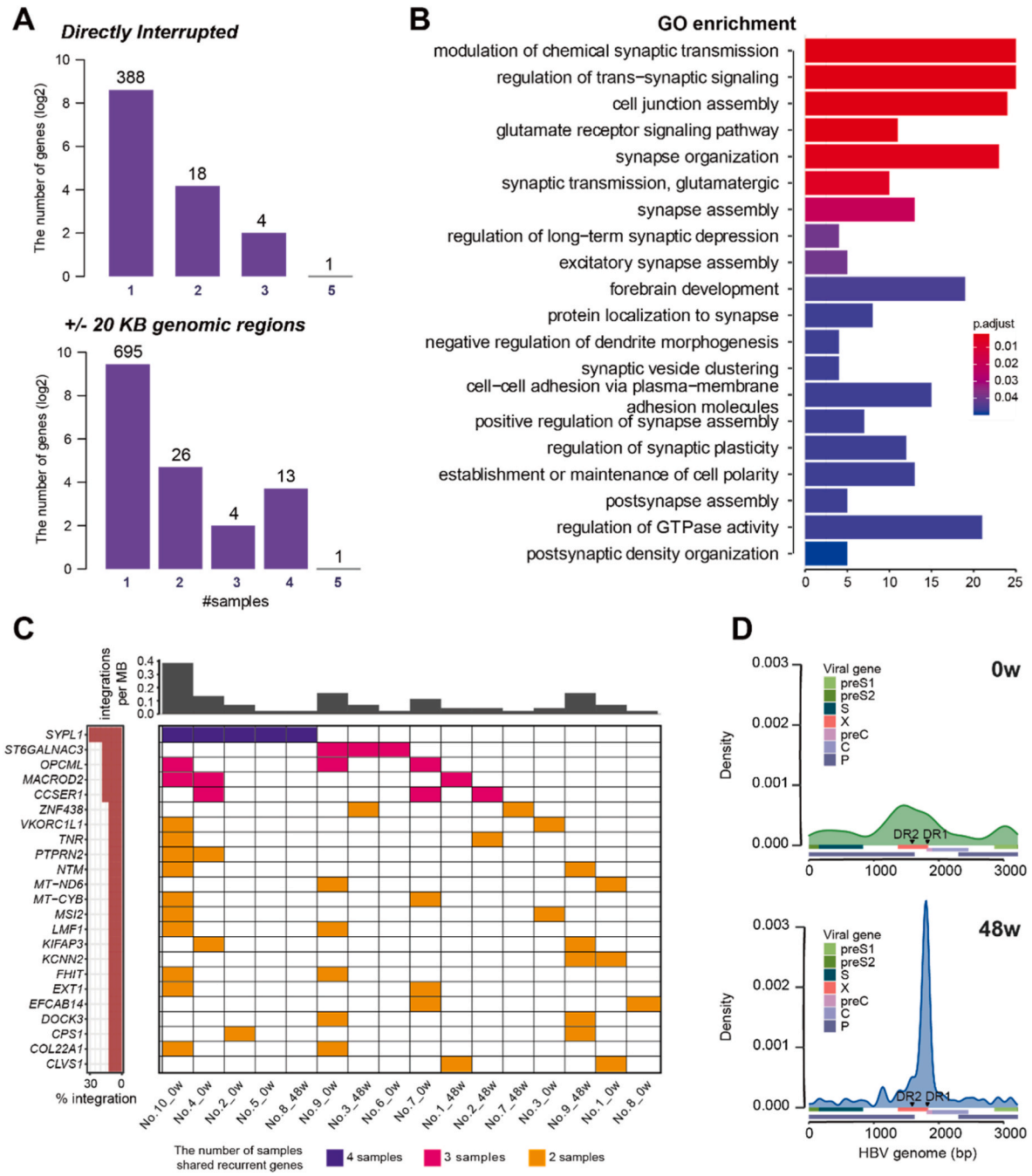

Fig. 2. Patterns of integrations of CHB patients before and after treatment. (A) The number of genes interrupted by HBV integration sites and the number of genes located within 20 kb upstream and downstream of integrations. X-axis represents the number of samples. Y axis represents the number of annotated genes in different number of samples. **(B)** GO enrichment analysis of 411 genes interrupted by HBV integration sites. **(C)** Waterfall plot summarizing the distribution of recurrent interrupted genes among different samples (genes observed in more than 1 sample). The purple box indicates the gene observed in 5 samples, the pink box indicates the gene observed in 3 samples, and the green box indicates it was observed in 2 samples. **(D)** The breakpoint distribution across the HBV genome of CHB patients before and after treatment.

Recurrent interrupted genes may exist in different patients, indicating potential hotspots in the host genome. Eighteen and four recurrent interrupted genes were shared by two and three samples, respectively (Fig. 2C). Here, the most common gene was the Synaptophysin-like 1 gene (*SYPL1*), which was detected in five samples (Fig. 2C). HBV Integrations interrupting *SYPL1* either located chr7: 105741915 or chr7: 105741918 in its intron 1 region, which was featured by the actively transcribed states (TxWk of chromHMM), indicating the chromatin open states (Fig. S2). In addition, patient No. 5 (after treatment) had one HBV integration (chr2: 216265486) in *FN1*, which is the hot-spot gene of HBV integrations in liver tissues adjacent to HCC.

Consistent with tumor HBV integrations, most viral breakpoints are located at nt 1600–1900 of the HBV genome, which harbors DR1 and DR2 as the dslDNA ending region (Chen et al., 2020). Seemingly, integration events detected after antiviral treatment were more likely to end exactly in this region (15/28, 53%, in samples before treatment, and 43/54, 79%, after treatment; Fig. 2D and Table S2).

Table 1
The annotated gene exist in the same CHB patient before and after treatment.

Gene	Sample no.	Treat	Chr	Pos	PB	HBV Pos[a]	HBV PB[a]
The overlap gene interrupted by HBV integration before and after treatment							
GLVS1	No.1	baseline	chr8	NA	62412274	NA	346(−)
		treatment	chr8	NA	62118869	NA	1792(+)
DOCK3	No.9	baseline	chr3	NA	51070499	NA	1381(−)
		treatment	chr3	50985393	NA	1792 (+)	NA
The overlap gene located 20 kb surrounding HBV integration before and after treatment							
FTCD	No.8	baseline	chr21	47554779	NA	1590 (+)	NA
COL6A2		treatment	chr21	47564173	NA	288 (+)	NA

[a] According to sequencing read mapping pattern, breakpoints with supported split junctions consistently ending at 3′ terminus had their human genome position listed as Pos, and those at 5′ end terminus as PB (paired breakpoints). Because both breakpoints may not be always found simultaneously, the missing one had the position listed as NA (Not available). See details for the pairing strategy in our previous study. (Chen et al., 2020).

3.3. Distinct genomic distribution of CHB integrations compared with those in HCC

Although the capture strategy is not a quantitative method of HBV integration, the integrations carried by a large population of affected cells tend to have high sequencing coverage (X). In comparison with previous tumor integrations, CHB integrations had much lower sequencing coverage, indicating that they were harbored by limited hepatocytes (~316X in previous tumor studies vs. ~15X in our baseline samples, $P < 2.2e^{-16}$; or vs. ~28X after treatment, $P < 2.2e^{-16}$, Wilcoxon rank-sum test; Fig. 3A). Tumor integrations were most likely to occur in chromosomes 5, 14, 19, and 21, whereas CHB integrations seemed to have no chromosome preference (Fig. 3B).

Annotation of DNase hypersensitivity and chromatin states (defined by chromHMM) revealed that (Fig. 3C and D), overall, host integration sites were more enriched in open active states (such as promoters) and more likely to have double-strand breaks as “fragile regions”, compared to chromatin inactive states (such as ChromHMM marks, RwprPCWk and Quies, Fig. S3). Tumor integrations had a higher enrichment score for open active states than CHB integrations, such as DNase, TssA, and ZNF/Rpts. However, integrations identified after ETV treatment had the lowest score (Fig. 3D, Fig. S2). Along with decreased integrations after antiviral treatment, the enrichment tendency of integrations in open chromatin regions and heterochromatin regions disappeared, with the enrichment score of heterochromatin decreasing from 0.30 at baseline to −0.21 after treatment. Additionally, tumor integrations are considered to have functional effects, with their enrichment in DNase regions (Enrichment Score is 1.78, *P-value* is 0.001). However, CHB integrations do not show this enrichment.

4. Discussion

HBV integration events are supposed to cause chromosomal instability, oncogenic activation, and inflammation (Cui et al., 2020; Zhao et al., 2020). Research efforts have focused on the causal relationship between HBV integration and liver cancer (Levrero and Zucman-Rossi, 2016; Mathkar et al., 2021). HBV integration can be found in the early stage of HBV infection (Chauhan et al., 2019; Tu et al., 2018), but rare attempts have been made to explore the effects of antiviral treatments on the changes in HBV integration profiles and their biological effects (Hu et al., 2018). Technical challenges exist particularly in analyzing chronically infected livers. Under current guidelines, liver biopsies are rarely performed, and the limited tissue obtained in each examination may not be adequate for diverse virological marker assays. Considering the excess of viral DNA probes in the capture assay examined in our previous study (Chen et al., 2020), all integrations in analyzed hepatocytes may be successfully detected. We did not observe a consistent reduction in integrations between paired samples from each patient, since individual differences in viral clearance and hepatocyte turnover in the liver may confound this attempt. However, the integration mechanism should be the same in all patients, and viral integrations could be taken as events occurring in a large population of hepatocytes before and after treatments. The overall reduction in integration events showed the suppressive role of ETV treatment, and their genomic features deserve attention.

We used ~200 ng DNA from one liver biopsy for each patient without accurate cell counts. The abundance of each integration could only be estimated according to its sequencing depth. As expected, clonal sizes of hepatocytes in CHB did not achieve the levels observed in advanced lesions, since clonal expansion may not be obvious at this stage. Clonal expansion occurred in patients with CHB, particularly for those over 40 years of age (Tu et al., 2015). In young patients with CHB but without liver cirrhosis (under 40 years of age), that was not the case.

Despite the aforementioned limitations, the contribution of integrations to serum HBsAg was evaluated from diverse aspects. First, the overall integration frequencies varied among patients. Moreover, more integrations may lead to high serum HBsAg level. Second, after ETV treatment, 60% of our patients almost achieved complete HBe loss (S/CO no more than 1, Table S1), and viral integrations were shown to significantly contribute to the HBsAg levels, particularly in particularly in HBeAg-negative CHB patients (Meier et al., 2021). Third, the viral coding ability of integrations was predicted following our previous strategy of pairing the ends for each integration event. The S protein-coding integrations, iHBV-S, can produce viral proteins or peptides in diverse previous studies (Zhang et al., 2021; Zhao et al., 2020). Their percentage in the HBV integration profile may be the major contributor to serum HBsAg level, and their consistent existence may explain the difficulties in controlling the HBsAg level by antiviral treatment, particularly in patients with fewer integrations detected. In this study, Patient 9 provided an example, in which although HBV replication was suppressed by antiviral treatment, HBsAg was not reduced to the same level in patients without iHBV-S integrations detected after therapy.

A previous study emphasized the tumor prevention effects of antiviral therapies (Hsu et al., 2020). HBV integrations have long been considered to be one of the carcinogenic factors during chronic infection (Mason et al., 2010; Tu et al., 2015; Xie et al., 2021). Our studies showed the reduced tendency of integration events after treatment using the nucleoside analogue, which may reduce the possibility of introducing deleterious changes into the host genome due to repressed HBV replication. Moreover, taking integrations of all patients with CHB before and after treatment, only one HBV integration site was found both before and after treatment. This indicates that after antiviral treatment, no clones experienced significant expansion during antiviral treatments. Although some recurrent integration genes were detected (eg. *STPL1*), these integration sites tend to be located at fragile genomic regions without necessarily interrupting tumor-related genes. The features of HBV integrations, including interrupted genes, enriched genomic regions or chromosomes, and open/close states of chromatins, are distinct among our CHB integrations and previous tumor ones. They may provide evidence that antiviral treatment could reduce tumor risk by influencing the viral integration profile of patients with CHB.

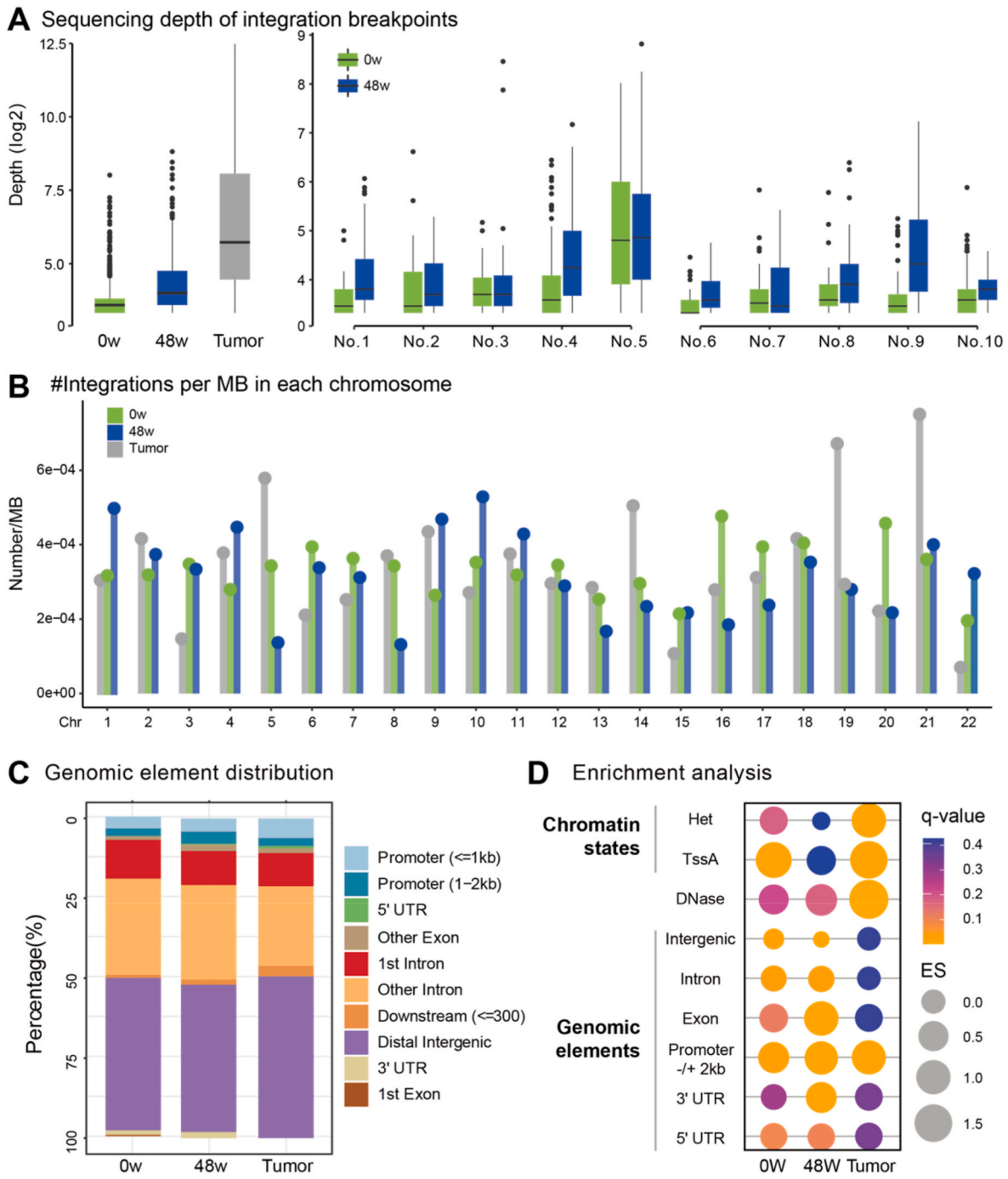

Fig. 3. Genome distribution of HBV integrations of patients with tumor and CHB. (A) The depth of HBV integration sites. The left panel shows the read depth of integrations of all the patients with tumors, and CHB patients before and after treatment. The right panel shows the read depth of integrations of 10 CHB patients before and after treatment. Baseline, CHB patient before treatment; Treatment: CHB patient after treatment. **(B)** The proportion of HBV integration sites located at human autosome. **(C)** The percentage of HBV integration sites located at different genomic elements of patients with tumor and CHB patients before and after treatment. (D) The enrichment of HBV integration sites located at different genomic elements and liver epigenomic features. TssA and Het were defined by chromHMM, in which TssA represents active TSS proximal promotes states and Het represents constitutive heterochromatin.

The study had some strengths and limitations. For strengths, first, regular blood collection and follow-up of all patients had been performed based on the strict procedures of the clinical trial. Second, comprehensive HBV-related virological markers were detected by the central laboratory, which may ensure an accurate effect evaluation of antiviral therapy. Third, liver samples were obtained before and after treatment, providing valuable clinical evidence. For limitations, first, the number of samples was relatively small. Therefore, more samples should be collected for validation. Second, the detection of integration sites by probe capture is not a quantitative method. Therefore, accurate accounting of hepatocytes is required for precise determination of integration frequency. Third, the prediction of viral integrants to evaluate viral protein ability relies on both integration breakpoints being detected. A low abundance of viral integrations in CHB liver tissues may cause only one breakpoint identified in the sequencing experiment, making HBV-S detection with limited sensitivity possible. Therefore, long-read sequencing may be helpful in further attempts, which can directly read through the integration sites, covering the flanking human

genomic regions and intact viral integrants (Xie et al., 2021). Fourth, longitudinal monitoring of the expansion process for clones carrying specific integrations may be helpful to elucidate the potential survival benefit of affected clones.

In summary, this is the first study DNA-capture profiling the HBV integrations in CHB patients before and after ETV treatment. Consistent with findings from previous studies, the serum HBsAg was correlated with HBV integrations in CHB patients, which could be complicated by the integration frequency, and viral protein-coding abilities of integrants. Notably, our study provides evidence that antiviral treatment may affect HBV integration profiles in CHB, particularly by reducing the integration occurrence. The distinct genomic features between integrations in CHB, especially after treatment, and tumor samples may indicate a decreasing risk of liver cancer occurrence benefit from antiviral therapy.

Author contributions

MYZ and HKZ performed experimental studies and drafted the manuscript. MYZ, HKZ, and XMC analyzed and interpreted the data. MYZ, XMW, HQX, XZG, and RHW performed the HBV virological tests. HKZ and DKZ contributed to the data generation and statistical analysis. DKZ, YCX, and JQN contributed to the experimental designs, interpreted data, and supervised the study. All authors reviewed the draft and performed a critical review of the manuscript.

Data availability statement

The original contributions presented in the study are included in the article/Supplementary Material. The data of this study are available from the corresponding author upon request.

Funding

This work was supported by the National Natural Science Foundation of China (project no. 81971936, 81201700), Fundamental Research Funds for the Central Universities, Hubei Province's Outstanding Medical Academic Leader Program, Gilead Sciences Research Scholars Program in Liver Disease Asia, Foundation for Innovative Research Groups of the Natural Science Foundation of Hubei (project no. 2020CFA015), Research and Innovation Team Project of Hubei Health Commission (project no. WJ2021C002), China Postdoctoral Science Foundation (project no. 2021TQ0026), Open Research Fund Program of the State Key Laboratory of Virology of China (2020KF006, 2022KF007), Higher Education Discipline Innovation Project (the 111 Project No. B13003), First Hospital of Jilin University, and Youth Development Foundation (JDYY11202018). These funders were not involved in the design of the study.

Declaration of competing interest

All of the authors declare no conflicts of interest and have submitted the ICMJE Form for Disclosure of Potential Conflicts of Interest.

Acknowledgments

We are grateful to the following professors—Yu L, Chen YP, Shang J, Liu LG, Zhang SQ, Jiang YF, Zhang MX, Tong QX, Zhang LL, Tan YW, Ma AL, Dang SS, Xu B, Jin ZJ, Li J, and Li XB—for their selfless help in the process of collecting and treating clinical cases.

Appendix A. Supplementary data

Supplementary data to this article can be found online at https://doi.org/10.1016/j.antiviral.2022.105363.

References

Beck, J., Nassal, M., 2007. Hepatitis B virus replication. World J. Gastroenterol. 13, 48–64.
Block, T.M., Gish, R., Guo, H., Mehta, A., Cuconati, A., Thomas London, W., Guo, J.T., 2013. Chronic hepatitis B: what should be the goal for new therapies? Antivir. Res. 98, 27–34.
Block, T.M., Guo, H., Guo, J.T., 2007. Molecular virology of hepatitis B virus for clinicians. Clin. Liver Dis. 11, 685–706 vii.
Chauhan, R., Shimizu, Y., Watashi, K., Wakita, T., Fukasawa, M., Michalak, T.I., 2019. Retrotransposon elements among initial sites of hepatitis B virus integration into human genome in the HepG2-NTCP cell infection model. Cancer Genet 235–236, 39–56.
Chen, W., Zhang, K., Dong, P., Fanning, G., Tao, C., Zhang, H., Guo, S., Wang, Z., Hong, Y., Yang, X., Lai, S., Ding, H., Zhao, H., Zeng, C., Protzer, U., Zhang, D., 2020. Noninvasive chimeric DNA profiling identifies tumor-originated HBV integrants contributing to viral antigen expression in liver cancer. Hepatol Int 14, 326–337.
Chinese Society of Hepatology, C.M.A., 2019. [The guidelines of prevention and treatment for chronic hepatitis B (2019 version)]. Zhonghua Gan Zang Bing Za Zhi 27, 938–961.
Cui, X., Wei, W., Wang, C., Qi, Y., Qin, X., Huang, L., Li, W., 2020. Studies on the correlation between mutation and integration of HBV in hepatocellular carcinoma. Biosci. Rep. 40.
Fujimoto, A., Totoki, Y., Abe, T., Boroevich, K.A., Hosoda, F., Nguyen, H.H., Aoki, M., Hosono, N., Kubo, M., Miya, F., Arai, Y., Takahashi, H., Shirakihara, T., Nagasaki, M., Shibuya, T., Nakano, K., Watanabe-Makino, K., Tanaka, H., Nakamura, H., Kusuda, J., Ojima, H., Shimada, K., Okusaka, T., Ueno, M., Shigekawa, Y., Kawakami, Y., Arihiro, K., Ohdan, H., Gotoh, K., Ishikawa, O., Ariizumi, S., Yamamoto, M., Yamada, T., Chayama, K., Kosuge, T., Yamaue, H., Kamatani, N., Miyano, S., Nakagama, H., Nakamura, Y., Tsunoda, T., Shibata, T., Nakagawa, H., 2012. Whole-genome sequencing of liver cancers identifies etiological influences on mutation patterns and recurrent mutations in chromatin regulators. Nat. Genet. 44, 760–764.
Hsu, Y.C., Wong, G.L., Chen, C.H., Peng, C.Y., Yeh, M.L., Cheung, K.S., Toyoda, H., Huang, C.F., Trinh, H., Xie, Q., Enomoto, M., Liu, L., Yasuda, S., Tanaka, Y., Kozuka, R., Tsai, P.C., Huang, Y.T., Wong, C., Huang, R., Jang, T.Y., Hoang, J., Yang, H.I., Li, J., Lee, D.H., Takahashi, H., Zhang, J.Q., Ogawa, E., Zhao, C., Liu, C., Furusyo, N., Eguchi, Y., Wong, C., Wu, C., Kumada, T., Yuen, M.F., Yu, M.L., Nguyen, M.H., 2020. Tenofovir versus entecavir for hepatocellular carcinoma prevention in an international consortium of chronic hepatitis B. Am. J. Gastroenterol. 115, 271–280.
Hu, B., Wang, R., Fu, J., Su, M., Du, M., Liu, Y., Li, H., Wang, H., Lu, F., Jiang, J., 2018. Integration of hepatitis B virus S gene impacts on hepatitis B surface antigen levels in patients with antiviral therapy. J. Gastroenterol. Hepatol. 33, 1389–1396.
Kim, S.W., Yoon, J.S., Lee, M., Cho, Y., 2021. Toward a complete cure for chronic hepatitis B: novel therapeutic targets for hepatitis B virus. Clin. Mol. Hepatol.
Lee, J.H., Ku, J.L., Park, Y.J., Lee, K.U., Kim, W.H., Park, J.G., 1999. Establishment and characterization of four human hepatocellular carcinoma cell lines containing hepatitis B virus DNA. World J. Gastroenterol. 5, 289–295.
Levrero, M., Zucman-Rossi, J., 2016. Mechanisms of HBV-induced hepatocellular carcinoma. J. Hepatol. 64, S84–S101.
Lin, S.Y., Su, Y.P., Trauger, E.R., Song, B.P., Thompson, E.G.C., Hoffman, M.C., Chang, T. T., Lin, Y.J., Kao, Y.L., Cui, Y., Hann, H.W., Park, G., Shieh, F.S., Song, W., Su, Y.H., 2021. Detection of hepatitis B virus-host junction sequences in urine of infected patients. Hepatol Commun 5, 1649–1659.
Martinez, M.G., Boyd, A., Combe, E., Testoni, B., Zoulim, F., 2021. Covalently closed circular DNA: the ultimate therapeutic target for curing HBV infections. J. Hepatol. 75, 706–717.
Mason, W.S., Liu, C., Aldrich, C.E., Litwin, S., Yeh, M.M., 2010. Clonal expansion of normal-appearing human hepatocytes during chronic hepatitis B virus infection. J. Virol. 84, 8308–8315.
Mathkar, P.P., Chen, X., Sulovari, A., Li, D., 2021. Characterization of hepatitis B virus integrations identified in hepatocellular carcinoma genomes. Viruses 13.
Meier, M.A., Calabrese, D., Suslov, A., Terracciano, L.M., Heim, M.H., Wieland, S., 2021. Ubiquitous expression of HBsAg from integrated HBV DNA in patients with low viral load. J. Hepatol. 75, 840–847.
Murakami, Y., Saigo, K., Takashima, H., Minami, M., Okanoue, T., Brechot, C., Paterlini-Brechot, P., 2005. Large scaled analysis of hepatitis B virus (HBV) DNA integration in HBV related hepatocellular carcinomas. Gut 54, 1162–1168.
Pollicino, T., Caminiti, G., 2021. HBV-integration studies in the clinic: role in the natural history of infection. Viruses 13.
Razavi, H., 2020. Global epidemiology of viral hepatitis. Gastroenterol. Clin. N. Am. 49, 179–189.
Ruan, P., Dai, X., Sun, J., He, C., Huang, C., Zhou, R., Cao, Z., Ye, L., 2019. Different types of viralhost junction found in HBV integration breakpoints in HBVinfected patients. Mol. Med. Rep. 19, 1410–1416.
Song, A., Lin, X., Chen, X., 2021. Functional cure for chronic hepatitis B: accessibility, durability, and prognosis. Virol. J. 18, 114.
Sung, W.K., Zheng, H., Li, S., Chen, R., Liu, X., Li, Y., Lee, N.P., Lee, W.H., Ariyaratne, P. N., Tennakoon, C., Mulawadi, F.H., Wong, K.F., Liu, A.M., Poon, R.T., Fan, S.T., Chan, K.L., Gong, Z., Hu, Y., Lin, Z., Wang, G., Zhang, Q., Barber, T.D., Chou, W.C., Aggarwal, A., Hao, K., Zhou, W., Zhang, C., Hardwick, J., Buser, C., Xu, J., Kan, Z., Dai, H., Mao, M., Reinhard, C., Wang, J., Luk, J.M., 2012. Genome-wide survey of recurrent HBV integration in hepatocellular carcinoma. Nat. Genet. 44, 765–769.
Tamori, A., Yamanishi, Y., Kawashima, S., Kanehisa, M., Enomoto, M., Tanaka, H., Kubo, S., Shiomi, S., Nishiguchi, S., 2005. Alteration of gene expression in human

hepatocellular carcinoma with integrated hepatitis B virus DNA. Clin. Cancer Res. 11, 5821–5826.
Tu, T., Budzinska, M.A., Shackel, N.A., Urban, S., 2017. HBV DNA integration: molecular mechanisms and clinical implications. Viruses 9.
Tu, T., Budzinska, M.A., Vondran, F.W.R., Shackel, N.A., Urban, S., 2018. Hepatitis B virus DNA integration occurs early in the viral life cycle in an in vitro infection model via sodium taurocholate cotransporting polypeptide-dependent uptake of enveloped virus particles. J. Virol. 92.
Tu, T., Mason, W.S., Clouston, A.D., Shackel, N.A., McCaughan, G.W., Yeh, M.M., Schiff, E.R., Ruszkiewicz, A.R., Chen, J.W., Harley, H.A., Stroeher, U.H., Jilbert, A. R., 2015. Clonal expansion of hepatocytes with a selective advantage occurs during all stages of chronic hepatitis B virus infection. J. Viral Hepat. 22, 737–753.
Wang, H., Men, P., Xiao, Y., Gao, P., Lv, M., Yuan, Q., Chen, W., Bai, S., Wu, J., 2019. Hepatitis B infection in the general population of China: a systematic review and meta-analysis. BMC Infect. Dis. 19, 811.
Wang, X., Chi, X., Wu, R., Xu, H., Gao, X., Yu, L., Liu, L., Zhang, M., Tan, Y., Niu, J., Jin, Q., 2021. Serum HBV RNA correlated with intrahepatic cccDNA more strongly than other HBV markers during peg-interferon treatment. Virol. J. 18, 4.
Wang, X., Wang, Z., Chi, X., Wu, R., Jin, Q., Xu, H., Gao, X., Yu, L., Chen, Y., Shang, J., Liu, L., Zhang, S., Jiang, Y., Zhang, M., Tong, Q., Zhang, L., Tan, Y., Ma, A., Dang, S., Xu, B., Jin, Z., Li, J., Li, X., Lu, F., Niu, J., 2020. Efficacy of a combination of HBV RNA and HBeAg in predicting HBeAg seroconversion in patients treated with entecavir for 144 weeks. Int. J. Infect. Dis. 99, 171–178.
Wooddell, C.I., Yuen, M.F., Chan, H.L., Gish, R.G., Locarnini, S.A., Chavez, D., Ferrari, C., Given, B.D., Hamilton, J., Kanner, S.B., Lai, C.L., Lau, J.Y.N., Schluep, T., Xu, Z., Lanford, R.E., Lewis, D.L., 2017. RNAi-based treatment of chronically infected patients and chimpanzees reveals that integrated hepatitis B virus DNA is a source of HBsAg. Sci. Transl. Med. 9.
Wu, T., Hu, E., Xu, S., Chen, M., Guo, P., Dai, Z., Feng, T., Zhou, L., Tang, W., Zhan, L., Fu, X., Liu, S., Bo, X., Yu, G., 2021. clusterProfiler 4.0: a universal enrichment tool for interpreting omics data. The Innovation 2 (3), 100141. https://doi.org/10.1016/j.xinn.2021.100141.
Xie, S., Leung, A.W., Zheng, Z., Zhang, D., Xiao, C., Luo, R., Luo, M., Zhang, S., 2021. Applications and potentials of nanopore sequencing in the (epi)genome and (epi) transcriptome era. The Innovation 2 (4), 100153. https://doi.org/10.1016/j.xinn.2021.100153.
Zhang, D., Zhang, K., Protzer, U., Zeng, C., 2021. HBV integration induces complex interactions between host and viral genomic functions at the insertion site. J Clin Transl Hepatol 9, 399–408.
Zhao, K., Liu, A., Xia, Y., 2020. Insights into hepatitis B virus DNA integration-55 Years after virus discovery. Innovation 1 (2), 100034. https://doi.org/10.1016/j.xinn.2020.100034.
Zhao, L.H., Liu, X., Yan, H.X., Li, W.Y., Zeng, X., Yang, Y., Zhao, J., Liu, S.P., Zhuang, X. H., Lin, C., Qin, C.J., Zhao, Y., Pan, Z.Y., Huang, G., Liu, H., Zhang, J., Wang, R.Y., Yang, Y., Wen, W., Lv, G.S., Zhang, H.L., Wu, H., Huang, S., Wang, M.D., Tang, L., Cao, H.Z., Wang, L., Lee, T.L., Jiang, H., Tan, Y.X., Yuan, S.X., Hou, G.J., Tao, Q.F., Xu, Q.G., Zhang, X.Q., Wu, M.C., Xu, X., Wang, J., Yang, H.M., Zhou, W.P., Wang, H. Y., 2016. Genomic and oncogenic preference of HBV integration in hepatocellular carcinoma. Nat. Commun. 7, 12992.